

Experimental Evidence of Dynamic Scaling in Colloidal Aggregation

Michael L. Broide and Richard J. Cohen

*Department of Physics, Massachusetts Institute of Technology, and Harvard-Massachusetts Institute of Technology
Division of Health Sciences and Technology, Cambridge, Massachusetts 02139*

(Received 19 July 1989)

We have studied the irreversible aggregation of colloidal polystyrene spheres during two limiting regimes of growth: diffusion-limited aggregation and reaction-limited aggregation. For each growth regime, the time-dependent cluster-size distribution exhibits a scaling form which reveals intrinsic features of these growth processes.

PACS numbers: 64.60.Cn, 05.40.+j, 82.70.Dd

The self-assembling of subunits to form large aggregates is a phenomenon central to many natural and synthetic processes. Over the past decade there has been a growing interest in developing a unified description of such processes.¹ Stimulating this interest is the curious fact that many irreversible aggregation processes produce fractal aggregates—the structure of aggregates appears to be the same over a wide range of length scales. A prototype of such a process is colloidal aggregation. For a variety of colloidal systems, which include silica,²⁻⁴ gold,⁴ and polystyrene,^{4,5} two limiting regimes of irreversible aggregation have been observed: (1) diffusion-limited aggregation (DLA), in which every collision between particles results in the formation of a bond, and (2) reaction-limited aggregation (RLA), in which only a small fraction of particle collisions leads to the formation of a bond. Each regime is characterized by distinctly different values for the fractal dimension d_f and distinctly different behavior for the kinetics of growth.

In this Letter, we describe a series of unique measurements of the kinetics of colloidal aggregation. These measurements utilize a single-particle light-scattering technique, which allows us to determine cluster-size distributions throughout the course of both DLA and RLA. For each regime of growth, we find that the cluster-size distribution exhibits dynamic scaling. That is, at long times t , the concentration of clusters composed of n subunits $c_n(t)$ approaches the factored form

$$c_n(t) \rightarrow s^{-2} \phi(n/s), \quad (1)$$

where $s(t)$ is related to the number-average mean cluster size, and $\phi(x)$ is the time-independent scaled distribution. For DLA, $\phi(x)$ is bell shaped with a peak occurring at $x \approx 0.1$, and $s(t) \sim t$. In contrast, for RLA, $\phi(x)$ decreases monotonically with x , and in particular, $\phi(x < 1) \sim x^{-1.5}$; $s(t) \sim t^2$. From these observations, we deduce features of the microscopic mechanisms which govern DLA and RLA.

We interpret our data in terms of Smoluchowski's

coagulation equation:⁶

$$\frac{dc_n}{dt} = \frac{1}{2} \sum_{i+j=n} k_{ij} c_i c_j - c_n \sum_{i=1}^{\infty} k_{ni} c_i,$$

where k_{ij} is the rate coefficient, or kernel, which parametrizes the rate that i -mers bond to j -mers. It is convenient to define dimensionless variables: $X_n \equiv c_n/c_0$, $T \equiv t/t_{\text{agg}}$, and $K_{ij} \equiv 2k_{ij}/k_{11}$, where $c_0 \equiv \sum_{n=1}^{\infty} n c_n$ is the total concentration of monomeric units in solution, and $t_{\text{agg}} \equiv 2/c_0 k_{11}$.

The coagulation equation has been solved exactly for simple forms of the kernel. To determine $X_n(T)$ for more complex forms of the kernel, one parametrizes the kernel in terms of two exponents λ and μ .⁷

$$K_{aij} \approx a^\lambda K_{ij}, \quad K_{i \ll j} \propto i^\mu j^{\lambda-\mu},$$

where a is a large positive constant. In this Letter, we consider only kernels with $\lambda \leq 1$ (nongelling kernels). For n and T large, solutions to the coagulation equation exhibit the dynamic scaling form, Eq. (1), which we observe in our data. The morphologies of $\phi(x)$ depend critically on the sign of μ . For kernels with $\mu < 0$, $\phi(x)$ is a bell-shaped function, while for kernels with $\mu \geq 0$, $\phi(x)$ decreases monotonically with x .

Our objective in this study is to determine the values of λ and μ for the DLA and RLA kernels based on the behavior of $s(T)$ and $\phi(x)$.

The experimental system consists of an aqueous suspension of surfactant-free charged polystyrene microspheres, 0.258 μm in radius, which are induced to irreversibly aggregate by the addition of salt (MgCl_2). The negative charge which each sphere bears arises from carboxyl groups on the surface of the spheres; these groups are fully ionized at $\text{pH} = 7$, the pH of our experiments. Spheres are manufactured by Interfacial Dynamics Corporation (Portland, Oregon; batch No. 10-23-78). For high concentrations of salt, the electrostatic repulsion between spheres is screened and aggregation proceeds at a rate near the Brownian collision rate of the spheres; $t_{\text{agg}}(\text{Brownian}) = 3\eta/4kTc_0$, where kT is the

thermal energy, and η is the solvent viscosity.⁶ This fast regime of aggregation corresponds to DLA. For lower concentrations of salt, the repulsion between spheres is only partially screened and aggregation proceeds at a rate slower than the Brownian collision rate. This slower regime of aggregation represents RLA.

At regular intervals of time, a small portion of the aggregating sample was removed from the reaction vessel and analyzed. In general, these aliquots were diluted in water prior to analysis, which halts the aggregation process. Control studies indicate that this dilution does not change the size distribution; spheres bind to one another irreversibly in our system. All experiments were performed at room temperature $22 \pm 0.8^\circ\text{C}$. The near equality of the densities of polystyrene and water prevents appreciable gravitational settling of clusters during the course of the experiments.

Cluster-size distributions were measured using a single-particle light-scattering technique.⁸ In this technique, clusters are constrained to flow single file past a focused laser beam; as each cluster traverses the beam, it scatters a pulse of light whose forward intensity is monotonically related to the cluster's mass. The high count rate of this technique (~ 100 clusters/sec) allows us to obtain distributions representing 10^4 clusters within minutes. Control studies indicate that our measurement technique does not shear clusters apart.⁹

At present, we can resolve clusters sizes up to $n=20$. For a highly aggregated sample, many clusters are larger than this limit; however, their presence does not hamper our ability to resolve clusters with $n=1-20$. Thus, we are able to record the temporal evolution of clusters with $n=1-20$ over very long periods of time. In addition, even though we are unable to determine the size of clusters larger than $n=20$, we are able to record their abun-

dance. This means we can determine $\sum_{n=1}^{\infty} c_n$, the total concentration of all clusters in the suspension, which is related to the number-average mean cluster size $\bar{n}_n \equiv c_0 / \sum_{n=1}^{\infty} c_n$. The quantity \bar{n}_n is related to $s(T)$; it is a key parameter for constructing $\phi(x)$ and for determining the value of λ .

For the DLA studies, $c_0 = 1.6 \times 10^8 / \text{cm}^3$ and $[\text{MgCl}_2] = 30 \text{ mM}$. These conditions result in $t_{\text{agg}} = 0.60 \text{ h}$, which we deduced from measurements of the initial rate of dimerization: $X_2(t \geq 0) \approx t/t_{\text{agg}}$. Normalizing t_{agg} by $t_{\text{agg}}(\text{Brownian})$ yields the stability factor W : $W \equiv t_{\text{agg}}(\text{measured})/t_{\text{agg}}(\text{Brownian}) = 1.9$.

At long times, we find that DLA has the following behavior: $\bar{n}_n \sim T$ (Fig. 1); $X_n(T)$ decays faster than T^{-2} ,¹⁰ and $X_n(T)$ vs n develops a peak, whose location shifts towards larger n with time (Fig. 2). This peaking of distributions suggests that the kernel for DLA has $\mu < 0$. For kernels with $\mu < 0$, $s \sim \bar{n}_n$.¹¹ In Fig. 2, we plot $s^2 X_n$ vs n/s for eight representative distributions measured between $T \approx 1$ and $T \approx 90$. The fact that all the distributions align onto a time-independent master curve demonstrates that $X_n(T) \approx s^{-2} \phi(n/s)$: The master curve in Fig. 2 is $\phi(x)$. For $T < 1$, $X_n(T)$ does not scale. We stress that this data collapse occurs without the aid of adjustable parameters. The shape of $\phi(x)$ reflects intrinsic properties about the aggregation process. The bell shape of $\phi(x)$ demonstrates that the kernel for DLA indeed has $\mu < 0$.

We have tried other scaling forms, such as $\bar{n}_n^\theta X_n$ vs n/\bar{n}_n , with $\theta = 1.0, 1.5$, and 2.5 , but $\theta = 2.0$ correlates the data the best.

For kernels with $\mu < 0$ and $\lambda < 1$, the coagulation equation predicts $\bar{n}_n \sim T^{1/(1-\lambda)}$.^{7,11} Experimentally, we find that $\bar{n}_n \sim T$ for $T > 15$ (Fig. 1), implying $\lambda \approx 0$. The theoretical prediction for the large- x behavior of

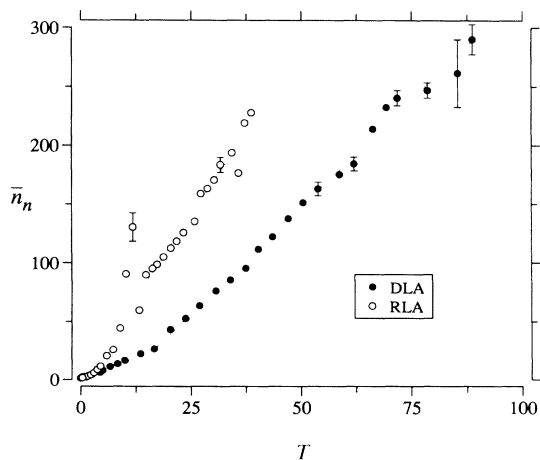


FIG. 1. Temporal evolution of the average cluster size for DLA and RLA. In both cases, for $T > 15$, \bar{n}_n grows linearly in time (dotted line).

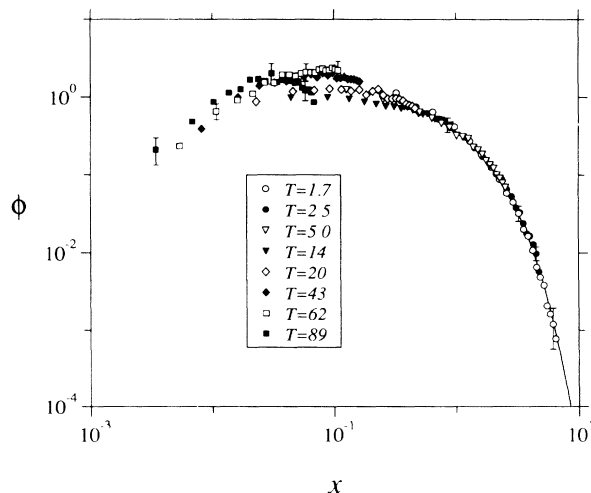


FIG. 2. Dynamic scaling plot for DLA showing alignment of distributions measured at different times. The solid line is the theoretical prediction for $\phi(x \gg 1)$ assuming $\lambda = 0$.

$\phi(x)$ also depends on λ : $\phi(x \gg 1) \sim x^{-\lambda} e^{-cx}$, where c is an adjustable parameter.⁷ Setting $\lambda = 0$ in this prediction results in a function which is consistent with our experimental data for $\phi(x > 1)$; see Fig. 2. In summary, our observations of $s(T)$ and $\phi(x)$ self-consistently imply that the DLA kernel has exponents $\mu < 0$ and $\lambda \approx 0$.

Our finding that $\lambda \approx 0$ is supported by other experiments of DLA.^{2,4,5} As a way of interpreting our results, we consider the Brownian kernel, which is believed to model the process of DLA:⁶

$$K_{ij} \sim (i^{1/d_f} + j^{1/d_f})(i^{-1/d_h} + j^{-1/d_h}),$$

where d_f is, again, the fractal dimension of the clusters and d_h is the hydrodynamic fractal dimension of the clusters. This kernel has exponents $\lambda = 1/d_f - 1/d_h$ and $\mu = -1/d_h < 0$. Assuming that the Brownian kernel indeed applies to DLA, our experimental finding $\lambda \approx 0$ implies $d_f \approx d_h$, in accord with direct measurements of d_f and d_h .¹²

For the RLA studies, $c_0 = 1.6 \times 10^{10}/\text{cm}^3$ and $[\text{MgCl}_2] = 7.5 \text{ mM}$. These conditions result in $t_{\text{agg}} = 1.4 \text{ h}$, and $W = 420$.¹³ For $T > 15$, we find that $\bar{n}_n \sim T$ (Fig. 1), and $X_n \sim T^{-1} n^{-\tau}$, where $\tau = 1.50 \pm 0.02$.¹⁰ This power-law decay for X_n vs n suggests that the kernel for RLA has $\mu \geq 0$. For distributions with $1 < \tau < 2$, $s \sim \bar{n}_n^{1/(2-\tau)}$.¹⁴ Assuming $\tau = 1.5$, we deduce that $s \sim \bar{n}_n^2$ for RLA. In Fig. 3, we plot $s^2 X_n$ vs n/s for eight representative distributions measured between $T \approx 1$ and $T \approx 40$. Just as in the case of the corresponding DLA plot, Fig. 2, the distributions align onto a time-independent master curve for $T > 1$. However, the shape of this curve is very different from the shape of the master curve for DLA. Changing the stability factor W not only changes the overall rate of aggregation, but also changes the form of the distribution.

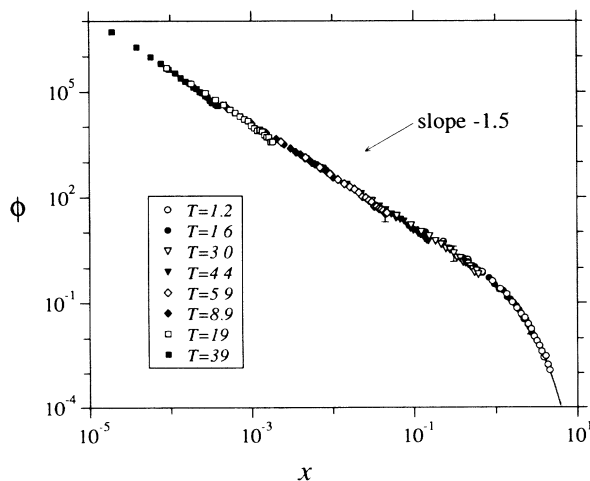


FIG. 3. Dynamic scaling plot for RLA showing alignment of distributions measured at different times. The solid line is the theoretical prediction for $\phi(x \gg 1)$ assuming $\lambda = \frac{1}{2}$.

We have tried using $s \sim \bar{n}_n$ to scale $X_n(T)$ for RLA, but this choice, which is valid for bell-shaped distributions or power-law distributions with $\tau < 1$, does not result in a data collapse.

For power-law size distributions with $1 < \tau < 2$, and for kernels with $\lambda < 1$, the scaling solution to the coagulation equation predicts that $\bar{n}_n \sim T^\omega$, where $\omega = (2 - \tau)/(1 - \lambda)$.¹¹ Experimentally, we find that $\bar{n}_n \sim T$ for $T > 15$ (Fig. 1), implying $\omega = 1$. With $\tau = 1.5$ and $\omega = 1$, the above expression for ω implies $\lambda = \frac{1}{2}$. The theoretical prediction for the large- x behavior of ϕ also supports the hypothesis $\lambda \approx \frac{1}{2}$. That is, $\phi(x \gg 1) \sim x^{-0.5} e^{-cx}$ is consistent with our experimental data for $\phi(x > 1)$; see Fig. 3. The small- x behavior of $\phi(x)$, $\phi(x \ll 1) \sim x^{-\tau}$, demonstrates that the RLA kernel has $\mu \geq 0$.⁷ Our finding that $X_n(T) \sim T^{-1}$ suggests that $\mu > 0$.¹⁵ For kernels with $\mu > 0$, the coagulation equation predicts $\tau = 1 + \lambda$.⁷ Experimentally, we find $\tau \approx 1.5$ (Fig. 3), implying $\lambda \approx \frac{1}{2}$. In summary, our observations self-consistently imply that the RLA kernel has exponents $\mu > 0$ and $\lambda \approx \frac{1}{2}$.

The dynamic scaling we observe in Figs. 2 and 3 is somewhat unexpected since it occurs for small n and for times prior to which $\bar{n}_n(T)$ develops its asymptotic form. It is possible that the scaled distributions we report, particularly the large- x portions of $\phi(x)$, may not represent the asymptotic forms for $\phi(x)$. However, the fact that distributions for both $T < 15$ and $T > 15$ align onto a single curve suggests that the $\phi(x)$ we measure is asymptotic. Furthermore, for monomeric initial conditions—the conditions used in our experiments—Hidy¹⁶ has shown that numerical solutions of the coagulation equation do indeed scale for small n and T , in support of our findings.

Our finding that $\tau \approx 1.5$ for RLA is consistent with other experiments of colloidal aggregation,^{4,17} although higher values of τ (1.8–2.0) have been reported.^{3,18} Our claim that $\lambda \approx \frac{1}{2}$ is supported by two recent experiments;^{19,20} however, several experiments of RLA²⁻⁵ find that the hydrodynamic radius, as determined by quasi-elastic light scattering, grows exponentially in time, which implies $\lambda = 1$. In addition, Ball *et al.*²¹ have proposed a theoretical model for the RLA kernel which supports the claim that $\lambda = 1$. We observe exponential growth of $\bar{n}_n(T)$ for $T < 6$, but this rapid growth crosses over into linear growth at later times. Perhaps the exponential growth observed by others slows down for aggregation times longer than those reported.

Meakin and Family²² have shown in simulations of RLA that the values of τ and λ depend on the details of the rate-limiting step in their simulation. Certain models lead to $\lambda \approx 1$, while others lead to $\lambda \approx \frac{1}{2}$. Perhaps the different types of aggregation kinetics observed in RLA experiments are due to differences in the rate-limiting step in each experimental system; solely specifying $W \gg 1$ may not uniquely define the aggregation kinetics.

A possibly significant difference in our system is that the monomers we use are 10 to 100 times larger than those used in most RLA experiments.

This work was supported by the National Science Foundation under Grant No. 8720308-CHE; Michael Broide is grateful for support from the Hertz Foundation.

¹*Kinetics of Aggregation and Gelation*, edited by F. Family and D. P. Landau (North-Holland, Amsterdam, 1984).

²C. Aubert and D. S. Cannel, *Phys. Rev. Lett.* **56**, 738 (1986).

³J. E. Martin, *Phys. Rev. A* **36**, 3415 (1987).

⁴M. Y. Lin, H. M. Lindsay, D. A. Weitz, R. C. Ball, R. Klein, and P. Meakin, *Proc. Roy. Soc. London A* **423**, 71 (1989).

⁵G. Bolle, C. Cametti, P. Codastefano, and P. Tartaglia, *Phys. Rev. A* **35**, 837 (1987).

⁶M. von Smoluchowski, *Z. Phys. Chem.* **92**, 129 (1917).

⁷P. G. J. van Dongen and M. H. Ernst, *Phys. Rev. Lett.* **54**, 1396 (1985).

⁸M. S. Bowen, M. L. Broide, and R. J. Cohen, *J. Colloid In-*

terface Sci. **105**, 605 (1985).

⁹M. L. Broide, Ph.D. thesis, Massachusetts Institute of Technology, 1988 (unpublished).

¹⁰M. L. Broide and R. J. Cohen (to be published).

¹¹T. W. Taylor and C. M. Sorensen, *Phys. Rev. A* **36**, 5415 (1987).

¹²P. Wiltzius, *Phys. Rev. Lett.* **58**, 710 (1987).

¹³This value of W is comparable to the conditions used in simulations of RLA [see P. Meakin and F. Family, *Phys. Rev. A* **38**, 2110 (1988)].

¹⁴This theoretical result is well known for kernels with $\lambda < 1$ (see, for example, Ref. 11); it is also true for $\lambda = 1$ (see Ref. 9).

¹⁵P. G. J. van Dongen and M. H. Ernst, *J. Phys. A* **18**, 2779 (1985).

¹⁶G. M. Hidy, *J. Colloid Sci.* **20**, 123 (1965).

¹⁷G. K. von Schulthess, G. B. Benedek, and R. W. DeBlois, *Macromolecules* **13**, 939 (1980).

¹⁸J. G. Rarity, R. N. Seabrook, and R. J. G. Carr, *Proc. Roy. Soc. London A* **423**, 89 (1989).

¹⁹J. P. Wilcoxon, J. E. Martin, and D. W. Schaefer, *Phys. Rev. A* **39**, 2675 (1989).

²⁰B. J. Olivier and C. M. Sorensen, *J. Colloid Interface Sci.* **134**, 139 (1990).

²¹R. C. Ball, D. A. Weitz, T. A. Witten, and F. Leyvraz, *Phys. Rev. Lett.* **58**, 274 (1987).

²²Meakin and Family, Ref. 13.